

Emergence and Disruption of Spin-Charge Separation in One-Dimensional Repulsive Fermions

Feng He^{1,2}, Yu-Zhu Jiang,¹ Hai-Qing Lin,^{3,4,*} Randall G. Hulet⁵, Han Pu,⁵ and Xi-Wen Guan^{1,6,7,†}

¹*State Key Laboratory of Magnetic Resonance and Atomic and Molecular Physics, Wuhan Institute of Physics and Mathematics, APM, Chinese Academy of Sciences, Wuhan 430071, China*

²*University of Chinese Academy of Sciences, Beijing 100049, China*

³*Beijing Computational Science Research Center, Beijing 100193, China*

⁴*Department of Physics, Beijing Normal University, Beijing 100875, China*

⁵*Department of Physics and Astronomy, and Rice Center for Quantum Materials, Rice University, Houston, Texas 77251-1892, USA*

⁶*Center for Cold Atom Physics, Chinese Academy of Sciences, Wuhan 430071, China*

⁷*Department of Theoretical Physics, Research School of Physics and Engineering, Australian National University, Canberra ACT 0200, Australia*



(Received 27 April 2020; accepted 17 September 2020; published 2 November 2020)

At low temperature, collective excitations of one-dimensional (1D) interacting fermions exhibit spin-charge separation, a unique feature predicted by the Tomonaga-Luttinger liquid (TLL) theory, but a rigorous understanding remains challenging. Using the thermodynamic Bethe ansatz (TBA) formalism, we analytically derive universal properties of a 1D repulsive spin-1/2 Fermi gas with arbitrary interaction strength. We show how spin-charge separation emerges from the exact TBA formalism, and how it is disrupted by the interplay between the two degrees of freedom that brings us beyond the TLL paradigm. Based on the exact low-lying excitation spectra, we further evaluate the spin and charge dynamical structure factors (DSFs). The peaks of the DSFs exhibit distinguishable propagating velocities of spin and charge as functions of interaction strength, which can be observed by Bragg spectroscopy with ultracold atoms.

DOI: 10.1103/PhysRevLett.125.190401

Interacting quantum many-body systems with rich internal degrees of freedom usually pose a formidable challenge for theoretical study. Understanding how interactions between fermions affect the state of a quantum liquid at low temperatures has been an important topic for over fifty years, and many outstanding questions still remain. A wealth of approximate formalism has been developed to understand the universal low-energy physics. These include Landau's Fermi liquid theory [1,2], the density matrix renormalization group [3,4], the Green's function approach [5], etc. In particular, the Tomonaga-Luttinger liquid (TLL) theory [6–10] describes the universal low-energy physics of strongly correlated systems in one dimension. The TLL usually refers to the collective motion of bosons that is significantly different from the free fermion nature in the Fermi liquid.

A hallmark of 1D physics is the splitting of low-lying excitations of interacting fermions into two separate TLLs, i.e., the separated quasiparticles carry either spin or charge. This phenomenon is known as spin-charge separation. Usually, TLL physics can be directly obtained from the Bethe ansatz (BA) solutions [11–14], where the particle-hole excitations have the same energy for a given momentum. This special feature of the TLL, however, is disrupted

once backward scattering is included or when the system is strongly disturbed by thermal fluctuations at quantum criticality [15,16]. Although the realizations of 1D cold atom systems [17–25] have confirmed many predictions from exactly solvable models, including recent studies on the dynamical deconfinement of spin and charge on 1D lattices [26–29], an observation of the unique spin-charge separation still remains a long-standing challenge in experiments [30–35]. We naturally ask if spin-charge separation, its criticality, and behavior beyond the TLL can be observed in ultracold atoms in a well-controlled manner.

In this Letter, we aim to answer these questions and report on the universal properties of spin-charge separated and disrupted liquids in a repulsive spin-1/2 Fermi gas. We present analytical results of thermodynamic and magnetic properties of the system which essentially mark the spin-charge separated liquids below a lower critical temperature, the universal scaling behavior of free fermion quantum criticality above an upper critical temperature, and the disrupted quantum liquids in between. We also evaluate exact low-lying excitations that indicate the separation of the particle-hole continuum in the charge sector from the two-spinon spectrum in the spin sector. Such separated spectra are exploited to calculate the charge and spin

dynamic structure factors (DSFs) and to probe the emergent phenomena such as spin-charge separation and fractional excitations in Fermi gases.

Yang-Gaudin model.—The Hamiltonian of the 1D δ function interacting Fermi gas, the so-called Yang-Gaudin model [36,37], is given by

$$\mathcal{H} = -\sum_{i=1}^N \frac{\partial^2}{\partial x_i^2} + 2c \sum_{1 \leq i < j \leq N} \delta(x_i - x_j) - HM - \mu N, \quad (1)$$

where the total number of particles N and the magnetization $M = (N_\uparrow - N_\downarrow)/2$ are defined by the numbers of spin-up N_\uparrow and spin-down N_\downarrow fermions, H and μ denote the external magnetic field and the chemical potential, respectively. All quantities in Eq. (1) are dimensionless where we have adopted a units system with $\hbar = 2m = 1$, here m is the mass of the particle. We also define the number density $n = N/L$ (L being the length of the system).

In this Letter we only consider the repulsive interaction with $c > 0$. The whole set of the exact BA wave functions, spectra and the associated BA equations were obtained by Yang in 1967 [36].

The universal properties of the system can be derived from the thermodynamic Bethe ansatz (TBA) equations which, for the repulsive Fermi gas, are given by [38–40]

$$\varepsilon(k) = k^2 - \mu - \frac{H}{2} - T \sum_{n=1}^{\infty} a_n * \ln[1 + e^{-\phi_n(\lambda)/T}], \quad (2)$$

$$\begin{aligned} \phi_n(\lambda) = & nH - T a_n * \ln[1 + e^{-\varepsilon(k)/T}] \\ & + T \sum_{m=1}^{\infty} T_{mn} * \ln[1 + e^{-\phi_m(\lambda)/T}], \end{aligned} \quad (3)$$

where $*$ denotes the convolution, $\varepsilon(k)$ and $\phi_n(\lambda)$ are the dressed energies for the charge and the length- n spin strings, respectively, with k 's and λ 's being the rapidities; the integral kernel $a_n(k) = (1/2\pi)\{(nc)/[(nc)^2/4 + k^2]\}$, and the functions T_{mn} are given in Refs. [12,40] (also see Supplemental Material [41] for more detail). Once $\varepsilon(k)$ is obtained, we can calculate the pressure, i.e., the equation of state $p = (T/2\pi) \int_{-\infty}^{\infty} \ln[1 + e^{-\varepsilon(k)/T}] dk$, from which all other thermodynamic quantities of interest can be obtained [41]. The TBA equations (2) and (3) reveal the full spin and thermal fluctuations controlled by the interplay between spin and charge.

Phase diagram and spin-charge separation.—Based on the configurations of spin orientations, the ground state phase diagram of a 1D repulsive Fermi gas in the $\tilde{\mu}$ - \tilde{H} plane contains three phases: vacuum, a mixed phase, and a fully polarized phase. The Wilson ratio, defined as $R_W^\chi = (4/3)[\pi k_B / (g\mu_B)]^2 [\chi / (c_V/T)]$, where χ is the magnetic susceptibility and c_V the specific heat, captures the essence of the quantum liquid [16,42,43]. This ratio becomes temperature-independent in the TLL regime,

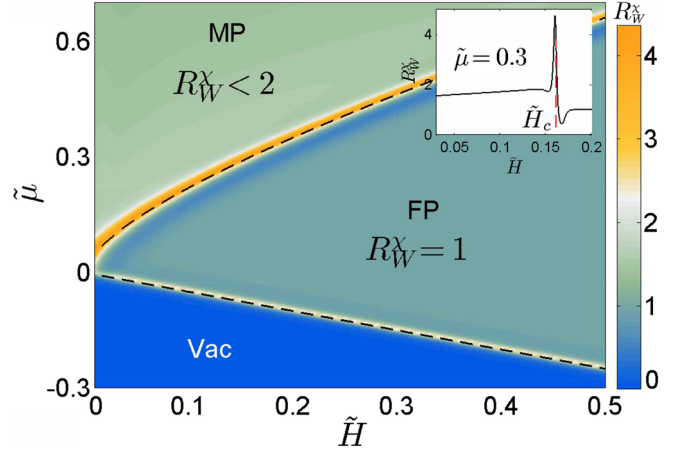


FIG. 1. (a) Contour plot of the Wilson ratio (WR) in the $\tilde{\mu} - \tilde{H}$ plane for the repulsive Fermi gas at $\tilde{T} = 0.005$. Here the dimensionless quantities are $\tilde{T} = (T/|c|^2)$, $\tilde{\mu} = (\mu/|c|^2)$, $\tilde{H} = (H/|c|^2)$. The values of the WR given by Eq. (4) elegantly mark three quantum phases: mixed phase (MP), full-polarized phase (FP), and vacuum at zero temperature. At low temperatures, the phase boundaries are indicated by sudden enhancements of the WR, which match well with the zero temperature phase boundaries (black dashed lines). The inset shows the WR vs magnetic field \tilde{H} at $\tilde{\mu} = 0.3$ and $\tilde{T} = 0.005$, where a sudden enhancement of the WR is observed.

while it displays a universal scaling behavior in the vicinity of the quantum critical point, signaling a breakdown of the TLL. We show that the WR elegantly marks the low-temperature phase diagram, as can be seen in Fig. 1, and characterizes the TLL of spinons via the following relation [44]

$$R_W^\chi = \frac{2v_c}{v_s + v_c} K_s. \quad (4)$$

Here the Luttinger parameter $K_s = 1$ at critical point and $K_s < 1$ in the MP phase. $R_W^\chi = 1$ for the FP phase. For the MP phase, we have $R_W^\chi < 2$, where the spin and the charge degrees of freedom dissolve into two separate TLLs with different speeds of propagation v_s and v_c , respectively.

The spin-charge separation phenomenon for the Fermi gas describes a splitting of low-energy excitations in the spin and the charge sectors. Because of the limited capabilities to control interaction, spin density, and temperature, unambiguously identifying the spin-charge separation is extremely challenging. Next, we derive rigorous results of spin-charge separation by means of the TBA equations (2) and (3) near and far from the quantum critical point (QCP) that separates the MP and the FP phases.

Throughout the MP phase with $\tilde{H} < \tilde{H}_c$, where \tilde{H}_c is the critical field for a fixed chemical potential (Fig. 1), we rigorously show [41] that the pressure can, in general, be given by

$$p - p_0 = \frac{\pi T^2}{6} \left(\frac{1}{v_c} + \frac{1}{v_s} \right), \quad (5)$$

where $p_0 = \int_{-k_0}^{k_0} \varepsilon(k) dk$ is the pressure at $T = 0$ and the charge and spin velocities are given by

$$v_c = \frac{t_c}{2\pi\rho_c(k_0)}, \quad v_s = \frac{t_s}{2\pi\rho_s(\lambda_0)}, \quad (6)$$

respectively, with $\rho_{c,s}$ being the distribution functions at the Fermi points k_0 and λ_0 for the charge and the spin sector, (i.e., the points at which the dressed energies vanish), respectively; and t_c and t_s are the respective linear slopes of the dispersion at the Fermi points. We show that v_c and v_s vary as functions of the external field H for a fixed chemical potential. More detail is given in the Supplemental Material [41].

Quantum criticality and disrupted liquids.— Understanding quantum criticality and the disrupted Luttinger liquid provide a rich paradigm for many-body physics. In contrast to the spinless Bose gases [23], the interplay between the spin and the charge degrees of freedom dramatically alters the critical behavior of the system. For $c \rightarrow \infty$, the states of the system are highly degenerate and the spin sector becomes an incoherent free spin chain that does not exhibit magnetic ordering [45]. Here we consider a system with arbitrary interaction strength to obtain the universality class of quantum criticality encoding the interplay between spin and charge. Using the TBA equations (2) and (3), we find that the phase transition occurs in the spin sector across the phase boundary between the MP and FP phases, see Ref. [41]. At finite temperatures, a quantum critical region (QC) fans out from the critical point, forming a critical cone in the \tilde{T} - \tilde{H} plane, see Fig. 2. In the QC region, all thermodynamic quantities can be cast into universal scaling forms. Through an expansion of the length-1 spin string dressed energy equation (2) and (3) with an arbitrary interaction strength at low temperatures, we obtain the universal scaling function for the equation of states (pressure) [41]

$$p - p_0 = \begin{cases} -gT^{3/2} \text{Li}_{\frac{3}{2}}(-e^{(s_0\Delta H/T)}), & \text{for } \mu = \mu_c, \\ -gT^{3/2} \text{Li}_{\frac{3}{2}}(-e^{(r_0\Delta\mu/T)}), & \text{for } H = H_c, \end{cases} \quad (7)$$

where $\Delta H = H_c - H$, $\Delta\mu = \mu_c - \mu$, $g = \arctan(2k_0/c)/[\pi^{3/2}\sqrt{a}]$, $s_0 = 1 - (1/\pi) \arctan[(2/c)k_0]$, $r_0 = -(2/\pi) \arctan[(2/c)k_0]$ and a is a constant determined by the critical chemical potential μ_c and the critical magnetic field H_c . Here the Fermi momentum $k_0 = \sqrt{\mu_c + H_c/2}$ is obtained from the charge dressed energy condition $\varepsilon(k_0) = 0$. The background pressure

$$p_0 = \begin{cases} \frac{\pi T^2}{6\sqrt{\mu_c + H/2}} + \frac{2}{3\pi}(\mu_c + H/2)^{3/2}, & \text{for } \mu = \mu_c, \\ \frac{\pi T^2}{6\sqrt{\mu + H_c/2}} + \frac{2}{3\pi}(\mu + H_c/2)^{3/2}, & \text{for } H = H_c, \end{cases} \quad (8)$$

reflects the regular part at quantum criticality. The correlation and dynamic critical exponents $\nu = 1/2$ and $z = 2$ are, respectively, read off by comparing Eq. (7) with the universal scaling form $p - p_0 = gT^{(1/z)+1} \mathcal{G}[(s_0\Delta H/T^{1/\nu z}), (r_0\Delta\mu/T^{1/\nu z})]$. These exponents also determine the two critical temperatures of the QC region $T_l^* = \alpha_1|H - H_c|^{\nu z}$ and $T_r^* = \alpha_2|H - H_c|$, indicated by the two black dashed lines in Fig. 2. Here $\alpha_{1,2} = s_0/y_{1,2}$ with $y_1 = -1.5629$, $y_2 = 3.6205$ are constants [44]. Building on the exact scaling form of the pressure (7), scaling functions of other thermodynamic quantities, such as magnetization, susceptibility, density, compressibility, and specific heat, can be evaluated in a straightforward way using standard statistical relations.

Our result, Eq. (7), provides not only a precise understanding of the emergent criticality of spinons interplaying with charge [41], but also insightful perspectives of disrupted liquids beyond TLL. The interplay between the spin and the charge degrees of freedom leads to large deviations from the linear dispersion in both the spin and the charge sectors and to the disruption of the TLL in the crossover region $E_{\text{spin}} \ll k_B T \ll E_F$, labeled as COR1 and COR2 in Fig. 2. Here E_{spin} and E_F are the energy of the spin sector and Fermi energy, respectively. The crossover region COR1 coincides with the so-called incoherent Luttinger liquid [46,47]. We observe from p_0 in Eq. (8) that the TLL nature only remains in the charge sector, while the dilute deconfined spinons become free fermionlike.

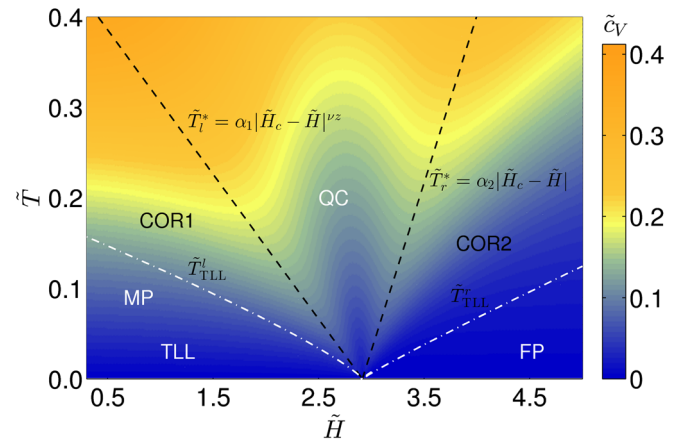


FIG. 2. Phase diagram in the \tilde{T} - \tilde{H} plane: contour plot of specific heat. We set the dimensionless chemical potentials $\tilde{\mu} = 2.5$, $\tilde{H}_c = 2.9145$. The black dashed lines denote the peak positions of specific heat, and the dot-dashed line shows the boundary of the linear T dependence of specific heat. The crossover regions between QC and the TLL are labeled as COR1 and COR2.

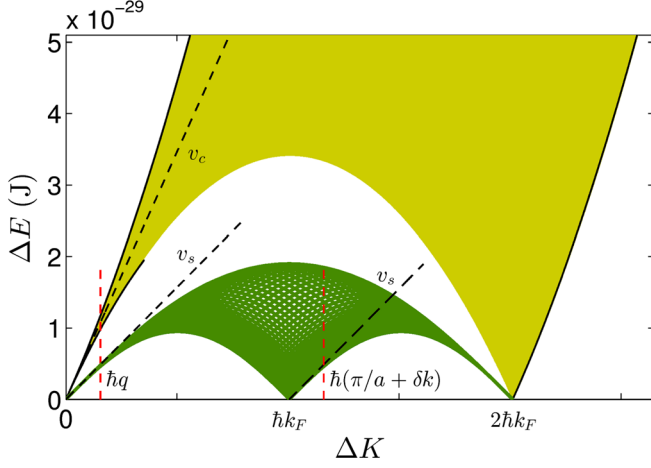


FIG. 3. Exact low energy excitation spectra in charge (yellow green) and spin (dark green) at $\gamma = c/n = 5.03$ ($a_s = 700a_0$) with the Fermi surface $k_F = n\pi$, density $n = N/L = 3 \times 10^6$ (1/m), $\Delta E = \hbar\omega$. The yellow green shows the particle-hole continuum excitation. The black solid lines indicate the thresholds of particle-hole excitation which remarkably manifest the free fermion-like dispersion (9) with an effective mass $m^* \approx 1.27m$ at low energy. The black dashed line in the charge excitation stands for the charge velocity v_c . The dark green shows the two-spin excitation, where the black dashed lines stand for the spin velocities v_s near $\Delta K = 0$ and $\hbar k_F$, respectively. The two red dashed lines indicate the positions of excitation momenta in charge and spin sectors for Fig. 4.

These CORs reveal a coexistence of liquid and gaslike states; for more details see Ref. [44].

Exact low-lying excitations and dynamic structure factor.—Solving the TBA equations (2) and (3), we obtain precisely the low-lying excitations in both spin and charge. As shown in Fig. 3, the excitations in the two sectors are separated from each other. The charge particle and hole excitations at low energy are given exactly by

$$\omega(q) = v_c|q| \pm \frac{\hbar q^2}{2m^*} + \dots \quad (9)$$

with $[m/(m^*)] = \{[\epsilon_c''(k_0)]/\{2[2\pi\rho_c(k_0)]^2\}\} - \{[\pi\rho_c'(k_0)\epsilon_c'(k_0)]/[2\pi\rho_c(k_0)]^3\}$, where m^* is the effective mass, taking the form $m^* \approx m[1 + (4 \ln 2/\gamma)]$ as $\gamma \gg 1$ [41]. For small q , the charge excitation can be well captured by the leading order in Eq. (9), while the second term is irrelevant. The charge DSF in a 1D repulsive Fermi gas has been recently measured [24,48] using the technique of Bragg spectroscopy [49,50], where the key feature of free Fermi liquid was observed in the DSF and the speed of sound in the charge sector was measured. The charge DSF of a free homogeneous Fermi gas is already known to be [51]

$$S(q, \omega) = \frac{\text{Im}\chi(q, \omega, k_F, T, N)}{\pi(1 - e^{-\beta\hbar\omega})}. \quad (10)$$

Based on the charge excitation spectrum (9), the interaction only modifies the effective mass with the Fermi point k_F replaced by $k_c = m^*v_c/\hbar$ [24]. As a consequence, it will move the resonance position from $\omega = v_F q$ to $\omega \approx v_c q$ in the excitation spectrum. Here we observe that for $T \rightarrow 0$, DSF $S(q, \omega) \neq 0$ only for $\omega_- \leq \omega \leq \omega_+$, where $\omega_{\pm} = v_c|q| \pm (\hbar q^2/2m^*)$ captures the dispersion (9). Taking the setting for a gas of spin-balanced ${}^6\text{Li}$ with particle number $N = 60$, several different values of interaction strength at temperature $T = 120$ nk, tube length $L = 20 \mu\text{m}$, and $q = 1.47 \mu\text{m}^{-1} \approx 0.15k_F$ [24,48], we demonstrate in Fig. 4(a) the Bragg spectrum as a function of Bragg frequency. The peak frequency of the DSF signal is plotted in Fig. 4(b) as a function of γ , from which we can read off the peak velocity defined as the ratio of peak frequency and q . As Fig. 4(b) demonstrates, this peak velocity is solely determined by the charge sound velocity, whereas the effective mass affects the width of the DSF. Our results on charge velocity and its dependence of the interaction strength are consistent with the experimental measurement and analysis reported in Ref. [24]. A more detailed study will be presented in the near future [44].

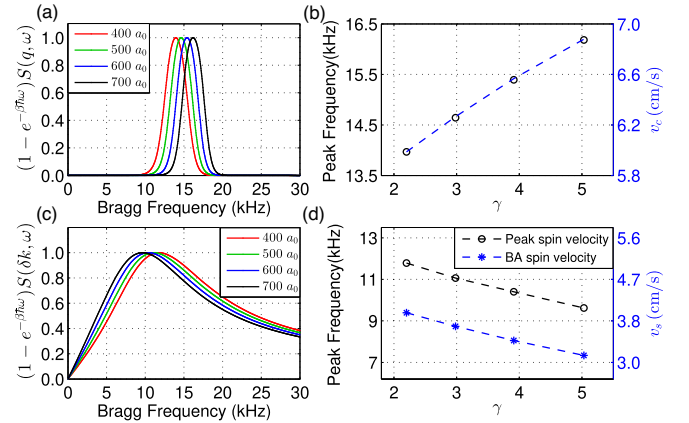


FIG. 4. Normalized charge and spin DSFs of a homogeneous Fermi gas with parameters corresponding to those of Ref. [24]: length $L = 20 \mu\text{m}$, particle numbers $N = 60$, temperature $T = 120$ nk, and various interaction strengths $a_s = 400a_0, 500a_0, 600a_0, 700a_0$. Here a_s is the 3D scattering length, which is related to the 1D interaction strength by $c = -2\hbar^2/ma_{1D}$ with $a_{1D} = (-a_{\perp}^2/2a_s)[1 - C(a_s/a_{\perp})]$ [52]. In converting to dimensional quantities, we have assumed the atoms are ${}^6\text{Li}$ with transverse harmonic confinement $\omega_{\perp} = (2\pi)198$ kHz. (a) Normalized charge DSF [Eq. (10)] vs Bragg frequency $\omega/2\pi$ at $q = 1.47 \mu\text{m}^{-1}$. (b) The empty circles denote the peak frequency of each spectrum vs γ . The corresponding peak charge velocity ω/q is given by the right axis. The dashed line is the charge sound velocity obtained from TBA. (c) Normalized spin DSF [Eq. (11)] vs Bragg frequency $\omega/2\pi$ at $\delta k = 1.47 \mu\text{m}^{-1}$. (d) The empty circles denote the peak frequency of each spectrum vs γ . The corresponding peak spin velocity $\omega/\delta k$ is given by the right axis. Stars are spin sound velocity obtained from the TBA.

In Fig. 3, we further show that the low-lying excitation in the spin sector gives rise to the two-spinon excitation, which remarkably displays the low-energy behavior of the Heisenberg spin-1/2 chain [41]. This two-spinon excitation spectrum holds for any finite interaction strength. The spin DSF of the Fermi gas is associated with the spin-spin correlation described by an effective Heisenberg spin chain. Near the Fermi momentum with wave number $\Delta K = \hbar(\pi/a + \delta k)$ with an effective lattice constant $a = L/N$, the spin DSF is given by [7,53,54]

$$S(\delta k, \omega) = \frac{1}{1 - e^{-\beta\hbar\omega}} \frac{A_{LL}}{k_B T} \text{Im} \left[\rho \left(\frac{\hbar\omega + v_s \hbar\delta k}{4\pi k_B T} \right) \times \rho \left(\frac{\hbar\omega - v_s \hbar\delta k}{4\pi k_B T} \right) \right], \quad (11)$$

where $\rho(x) = \Gamma(1/4 - ix)/\Gamma(3/4 - ix)$, and v_s is the spin velocity of the spin chain which can also be obtained from the second equation of (6) in the strong interaction limit. Also, $A_{LL} = -c_{\perp}^2 \alpha/2$ is a constant with the length scale parameter α and a constant factor c_{\perp} . With the same setting for the above charge DSF, we show in Figs. 4(c) and 4(d) the spin DSF signal and the spin peak velocity read off from its peak positions. As Fig. 4(d) shows, unlike in the charge case, here the peak velocity does not coincide with the spin sound velocity due to the peculiar feature of the two-spinon excitation near $\Delta K = \hbar\pi/a$ [41]. However, both the spin peak and the sound velocities are almost linearly decreasing functions of γ , in contrast to the charge velocity dependence on γ . This is a clear and unambiguous demonstration of the spin-charge separation. The fractional excitations beyond the two-spinon DSF (11) involve length- n spin strings (high order spinon process) in the spin imbalanced Fermi gas; see the TBA Eqs. (2) and (3).

Summary.—We have presented universal properties of the spin-charge separation and disrupted liquids at and off quantum criticality. The emergent liquid and gaslike quantum phases near QCP show a subtle interplay between the spin and charge degrees of freedom. The universal scaling functions, the crossover temperatures, as well as the DSFs deeply reveal the essence of the separated TLLs and their disruption, which takes us beyond the spin-charge separation paradigm. Our method suggests a promising way to control fractional spin excitations, TLLs, and magnetism in ultracold atomic systems with higher symmetries.

The authors thank Y. Y. Chen, S. Cheng, A. del Campo, and T. Giamarchi for helpful discussions. This work is supported by the key NSFC Grant No. 11534014, and NSFC Grants No. 11874393, No. 1167420, No. 11774390 and the National Key R&D Program of China No. 2017YFA0304500. H. Q. L. acknowledges financial support from National Science Association Funds

U1930402 and NSFC 11734002, as well as computational resources from the Beijing Computational Science Research Center. H. P. acknowledges supports from the U.S. NSF and the Welch Foundation (Grant No. C-1669). R. G. H. acknowledges support from an ARO MURI (Grant No. W911NF-14-1-0003), the U.S. NSF (Grant No. PHY-1707992), and the Welch Foundation (Grant No. C-1133).

*haiqing0@csrc.ac.cn

†xiwen.guan@anu.edu.au

- [1] G. Baym and C. Pethick, *Landau Fermi-Liquid Theory: Concepts and Applications* (John Wiley & Sons, New York, 2008).
- [2] D. Pines, *Theory of Quantum Liquids: Normal Fermi Liquids* (CRC Press, Boca Raton, 2018).
- [3] U. Schollwöck, The density-matrix renormalization group: A short introduction, *Phil. Trans. R. Soc. A* **369**, 2643 (2011).
- [4] C. Kollath, U. Schollwöck, and W. Zwerger, Spin-Charge Separation in Cold Fermi Gases: A Real Time Analysis, *Phys. Rev. Lett.* **95**, 176401 (2005).
- [5] E. N. Economou, *Green's Functions in Quantum Physics* (Springer, Heidelberg, 2006), Vol. 7.
- [6] F. D. M. Haldane, 'Luttinger liquid theory' of one-dimensional quantum fluids. I. Properties of the Luttinger model and their extension to the general 1D interacting spinless fermi gas, *J. Phys. C* **14**, 2585 (1981).
- [7] T. Giamarchi, *Quantum Physics in One Dimension*, International Series of Monographs on Physics (Oxford University Press, Oxford, 2003).
- [8] A. Imambekov, T. L. Schmidt, and L. I. Glazman, One-dimensional quantum liquids: Beyond the Luttinger liquid paradigm, *Rev. Mod. Phys.* **84**, 1253 (2012).
- [9] A. J. Schofield, Non-fermi liquids, *Contemp. Phys.* **40**, 95 (1999).
- [10] F. H. L. Essler, H. Frahm, F. Göhmann, A. Klümper, and V. E. Korepin, *The One-Dimensional Hubbard Model* (Cambridge University Press, Cambridge, 2005).
- [11] A. Recati, P. O. Fedichev, W. Zwerger, and P. Zoller, Spin-Charge Separation in Ultracold Quantum Gases, *Phys. Rev. Lett.* **90**, 020401 (2003).
- [12] J. Y. Lee, X.-W. Guan, K. Sakai, and M. T. Batchelor, Thermodynamics, spin-charge separation, and correlation functions of spin-1/2 fermions with repulsive interaction, *Phys. Rev. B* **85**, 085414 (2012).
- [13] M. Mestyán, B. Bertini, L. Piroli, and P. Calabrese, Spin-charge separation effects in the low-temperature transport of one-dimensional fermi gases, *Phys. Rev. B* **99**, 014305 (2019).
- [14] O. I. Pâtu, A. Klümper, and A. Foerster, Quantum critical behavior and thermodynamics of the repulsive one-dimensional Hubbard model in a magnetic field, *Phys. Rev. B* **101**, 035149 (2020).
- [15] S. Sachdev, *Quantum Phase Transitions* (Cambridge University Press, Cambridge, 2001).
- [16] X.-W. Guan, M. T. Batchelor, and C. Lee, Fermi gases in one dimension: From Bethe ansatz to experiments, *Rev. Mod. Phys.* **85**, 1633 (2013).

- [17] T. Kinoshita, T. Wenger, and D. S. Weiss, Observation of a one-dimensional Tonks-Girardeau gas, *Science* **305**, 1125 (2004).
- [18] T. Kinoshita, T. Wenger, and D. S. Weiss, A quantum newton's cradle, *Nature (London)* **440**, 900 (2006).
- [19] B. Paredes, A. Widera, V. Murg, O. Mandel, S. Fölling, I. Cirac, G. V. Shlyapnikov, T. W. Hänsch, and I. Bloch, Tonks-Girardeau gas of ultracold atoms in an optical lattice, *Nature (London)* **429**, 277 (2004).
- [20] E. Haller, M. Gustavsson, M. J. Mark, J. G. Danzl, R. Hart, G. Pupillo, and H.-C. Nägerl, Realization of an excited, strongly correlated quantum gas phase, *Science* **325**, 1224 (2009).
- [21] G. Pagano, M. Mancini, G. Cappellini, P. Lombardi, F. Schäfer, H. Hu, X.-J. Liu, J. Catani, C. Sias, M. Inguscio *et al.*, A one-dimensional liquid of fermions with tunable spin, *Nat. Phys.* **10**, 198 (2014).
- [22] Y.-a. Liao, A. S. C. Rittner, T. Paprotta, W. Li, G. B. Partridge, R. G. Hulet, S. K. Baur, and E. J. Mueller, Spin-imbalance in a one-dimensional fermi gas, *Nature (London)* **467**, 567 (2010).
- [23] B. Yang, Y.-Y. Chen, Y.-G. Zheng, H. Sun, H.-N. Dai, X.-W. Guan, Z.-S. Yuan, and J.-W. Pan, Quantum Criticality and the Tomonaga-Luttinger Liquid in One-Dimensional Bose Gases, *Phys. Rev. Lett.* **119**, 165701 (2017).
- [24] T. L. Yang, P. Grišins, Y. T. Chang, Z. H. Zhao, C. Y. Shih, Thierry Giamarchi, and R. G. Hulet, Measurement of the Dynamical Structure Factor of a 1D Interacting Fermi Gas, *Phys. Rev. Lett.* **121**, 103001 (2018).
- [25] M. Schemmer, I. Bouchoule, B. Doyon, and J. Dubail, Generalized Hydrodynamics on an Atom Chip, *Phys. Rev. Lett.* **122**, 090601 (2019).
- [26] J. Vijayan, P. Sompet, G. Salomon, J. Koepsell, S. Hirthe, A. Bohrdt, F. Grusdt, I. Bloch, and C. Gross, Time-resolved observation of spin-charge deconfinement in fermionic Hubbard chains, *Science* **367**, 186 (2020).
- [27] T. A. Hilker, G. Salomon, F. Grusdt, A. Omran, M. Boll, E. Demler, I. Bloch, and C. Gross, Revealing hidden anti-ferromagnetic correlations in doped Hubbard chains via string correlators, *Science* **357**, 484 (2017).
- [28] A. Bohrdt, D. Greif, E. Demler, M. Knap, and F. Grusdt, Angle-resolved photoemission spectroscopy with quantum gas microscopes, *Phys. Rev. B* **97**, 125117 (2018).
- [29] R. Emilio Barfknecht, A. Foerster, and N. Thomas Zinner, Dynamics of spin and density fluctuations in strongly interacting few-body systems, *Sci. Rep.* **9**, 15994 (2019).
- [30] C. Kim, A. Y. Matsuura, Z.-X. Shen, N. Motoyama, H. Eisaki, S. Uchida, T. Tohyama, and S. Maekawa, Observation of Spin-Charge Separation in One-Dimensional SrCuO₂, *Phys. Rev. Lett.* **77**, 4054 (1996).
- [31] O. M. Auslaender, H. Steinberg, A. Yacoby, Y. Tserkovnyak, B. I. Halperin, K. W. Baldwin, L. N. Pfeiffer, and K. W. West, Spin-charge separation and localization in one dimension, *Science* **308**, 88 (2005).
- [32] B. J. Kim, H. Koh, E. Rotenberg, S.-J. Oh, H. Eisaki, N. Motoyama, S. Uchida, T. Tohyama, S. Maekawa, Z.-X. Shen, and C. Kim, Distinct spinon and holon dispersions in photoemission spectral functions from one-dimensional SrCuO₂, *Nat. Phys.* **2**, 397 (2006).
- [33] Y. Jompoli, C. J. B. Ford, J. P. Griffiths, I. Farrer, G. A. C. Jones, D. Anderson, D. A. Ritchie, T. W. Silk, and A. J. Schofield, Probing spin-charge separation in a Tomonaga-Luttinger liquid, *Science* **325**, 597 (2009).
- [34] T. Giamarchi, Theory for 1D quantum materials tested with cold atoms and superconductors, *Physics* **10**, 115 (2017).
- [35] J. Vijayan, P. Sompet, G. Salomon, J. Koepsell, S. Hirthe, A. Bohrdt, F. Grusdt, I. Bloch, and C. Gross, Time-resolved observation of spin-charge deconfinement in fermionic Hubbard chains, *Science* **367**, 186 (2020).
- [36] C.-N. Yang, Some Exact Results for the Many-Body Problem in One Dimension with Repulsive Delta-Function Interaction, *Phys. Rev. Lett.* **19**, 1312 (1967).
- [37] M. Gaudin, Un système a une dimension de fermions en interaction, *Phys. Lett.* **24A**, 55 (1967).
- [38] C. K. Lai, Thermodynamics of Fermions in One Dimension with a δ -Function Interaction, *Phys. Rev. Lett.* **26**, 1472 (1971).
- [39] C. K. Lai, Thermodynamics of a one-dimensional system of fermions with a repulsive δ -function interaction, *Phys. Rev. A* **8**, 2567 (1973).
- [40] M. Takahashi, One-dimensional electron gas with delta-function interaction at finite temperature, in *Exactly Solvable Models Of Strongly Correlated Electrons* (World Scientific, Singapore, 1994), pp. 388–406.
- [41] See Supplemental Material at <http://link.aps.org/supplemental/10.1103/PhysRevLett.125.190401> for basic introduction to the Bethe ansatz equations for the 1D spin-1/2 Fermi gas and partial derivations of properties of the spin-charge separated and disrupted liquids.
- [42] K. G. Wilson, The renormalization group: Critical phenomena and the Kondo problem, *Rev. Mod. Phys.* **47**, 773 (1975).
- [43] X.-W. Guan, X.-G. Yin, A. Foerster, M. T. Batchelor, C.-H. Lee, and H.-Q. Lin, Wilson Ratio of Fermi Gases in One Dimension, *Phys. Rev. Lett.* **111**, 130401 (2013).
- [44] F. He, Y. Jiang, H.-Q. Lin, R. G. Hulet, H. Pu, and X.-W. Guan, Spin-charge separated and disrupted liquids: A comprehensive study (to be published).
- [45] M. Takahashi, *Thermodynamics of One-Dimensional Solvable Models* (Cambridge University Press, Cambridge, England, 2005).
- [46] G. A. Fiete, The spin-incoherent Luttinger liquid, *Rev. Mod. Phys.* **79**, 801 (2007).
- [47] V. V. Cheianov and M. B. Zvonarev, Nonunitary Spin-Charge Separation in a One-Dimensional Fermion Gas, *Phys. Rev. Lett.* **92**, 176401 (2004).
- [48] T.-L. Yang, Dynamical response of an interacting 1-dimensional Fermi gas, Ph. D. thesis, Rice University, 2018.
- [49] S. Hoinka, M. Lingham, M. Delehay, and C. J. Vale, Dynamic Spin Response of a Strongly Interacting Fermi Gas, *Phys. Rev. Lett.* **109**, 050403 (2012).
- [50] A. Brunello, F. Dalfovo, L. Pitaevskii, S. Stringari, and F. Zambelli, Momentum transferred to a trapped bose-einstein condensate by stimulated light scattering, *Phys. Rev. A* **64**, 063614 (2001).

- [51] A. Yu Cherny and J. Brand, Polarizability and dynamic structure factor of the one-dimensional bose gas near the Tonks-Girardeau limit at finite temperatures, *Phys. Rev. A* **73**, 023612 (2006).
- [52] M. Olshanii, Atomic Scattering in the Presence of an External Confinement and a Gas of Impenetrable Bosons, *Phys. Rev. Lett.* **81**, 938 (1998).
- [53] H.J. Schulz, Correlated fermions in one dimension, in *Exactly Solvable Models Of Strongly Correlated Electrons* (World Scientific, Singapore, 1994), pp. 198–215.
- [54] B. Lake, D.A. Tennant, J.-S. Caux, T. Barthel, U. Schollwck, S.E. Nagler, and C.D. Frost, Multispinon Continua at Zero and Finite Temperature in a Near-Ideal Heisenberg Chain, *Phys. Rev. Lett.* **111**, 137205 (2013).